Separation and Purification Technology 316 (2023) 123797

Contents lists available at ScienceDirect

Separation and Purification Technology

journal homepage: www.elsevier.com/locate/seppur

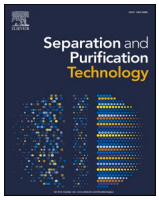

Simple gold recovery from e-waste leachate by selective precipitation using a quaternary ammonium salt

André F.M. Nogueira [a], Ana R.F. Carreira [a], Sílvia J.R. Vargas [a,b], Helena Passos [a], Nicolas Schaeffer [a,*], João A.P. Coutinho [a]

[a] CICECO - Aveiro Institute of Materials, Department of Chemistry, University of Aveiro, 3810-193 Aveiro, Portugal
[b] Purdue University, West Lafayette, IN 47907, United States

ARTICLE INFO

Keywords:
Recycling
Electronic waste
Molecular recognition
Circular economy
Ionic liquid

ABSTRACT

Precipitation processes, if selective, present a simple and economical alternative for the recovery of critical metals from primary and secondary ores including electronic wastes. In this work, the recovery of gold by precipitation from both mono-elemental solutions and real CPU leach solution was demonstrated using hydrophilic quaternary ammonium salts. The gold precipitation yield is shown to be dependent on the apolar volume of the precipitant, with the addition of tetrabutylammonium-based salts resulting in the recovery of over 90 % of gold from synthetic solutions. The origin of gold precipitation selectivity relative to common metal ions upon addition of tetrabutylammonium nitrate ($[N_{4444}][NO_3]$) was assigned by X-ray crystal structure to the formation of size selective apolar cavity between neighbouring $[N_{4444}]^+$ cation and the $[AuCl_4]^-$ anion. Following optimisation as a function of the gold to precipitant molar ratio, *aqua regia* concentration and time, approximately 70 % of gold could be recovered from waste CPU leach solution with a final purity of 91.4 % (mol/mol). $[N_{4444}][NO_3]$ proved to be a versatile gold extractant and could be further applied as part of an acidic aqueous biphasic system at higher *aqua regia* concentrations were precipitation yields decreased, ensuring a selective gold recovery across a range of leachate conditions. The disclosed results improve the circularity of gold by providing a new avenue for its simple recycling.

1. Introduction

The recovery of gold (Au) from ores is of economic and environmental importance, not only due to its perceived artistic and monetary value but by also being a crucial element in catalysis, nanotechnology, and modern electronics.[1] In this context, secondary "urban" ores such as electronic wastes are of particular interest as their Au content is one to two order of magnitude greater than in mined ores.[2,3] For example, waste printed circuit boards (PCBs) contain on average 224 ppm of Au [4] compared to 18 ppm in ores,[5] with Au representing over 50 % of the inherent metal value of PCBs.[2] The resource perspective for the globally generated secondary raw materials of e-waste in 2019 is estimated at 57×10^9 US$, of which only 10×10^9 US$ are currently being valorised to some extent.[3] Considering the anticipated increase in the yearly production of e-waste from 53.6×10^6 tons in 2019 to 74.7×10^6 tons in 2030,[3] and that the Au content present in e-waste represents approximately 9–11 % of its global annual mine production,[6,7] there is a clear onus for the simple and effective Au recovery from e-waste. Gold recycling is expected to improve supply chain sustainability by diminishing supply risk and to support the development of a circular economy. Nevertheless, the heterogeneity of e-waste compounded by the low Au concentration relative to other metals requires highly selective approaches which often comes at the expense of process complexity, cost, and environmental impact.

Adsorption using activated carbon (Carbon-in-Pulp process) and cementation using zinc (Merrill–Crowe process) represent the current industrial options for the recovery of Au from low concentration cyanide solutions.[8] Although these processes are generally efficient and cost-effective, they present limitations in the treatment of low-grade and complex ores. Furthermore, alternatives to cyanidation are actively pursued due to its well documented toxicity.[9] Recently, more sophisticated complexing agents were used for the molecular recognition of square planar haloaurate anions using either supramolecular or host–guest chemistry.[5] Examples include α-cyclodextrin capable of

* Corresponding author.
E-mail address: nicolas.schaeffer@ua.pt (N. Schaeffer).

https://doi.org/10.1016/j.seppur.2023.123797
Received 13 February 2023; Received in revised form 3 April 2023; Accepted 4 April 2023
Available online 7 April 2023

selectively forming insoluble molecular superstructures with $[AuX_4]^-$ (X = Cl/Br) and alkali metals in solution,[10,11] and the nearly instantaneous precipitation of $[AuX_4]^-$ using cucurbit [6] uril (CB [6]) through the formation of 1D (in the case of $[AuCl_4]^-$ precipitation) or 2D (for $[AuBr_4]^-$) solid-state superstructures capable of embedding the gold anions.[6] Additionally, a number of aromatic and aliphatic amides were shown to form supramolecular assemblies suitable for $[AuCl_4]^-$recognition upon protonation, allowing for gold precipitation from simple solutions [12] and e-waste leachates [13,14] through the formation of insoluble, infinitely extended structures. Similarly, 1-alkyl-1-methylpiperidinium ($[C_x mpip]^+$) and 1-alkyl-3-methylimidazolium ($[C_x mim]^+$) chloride ionic liquids (ILs) could precipitate $[AuX_4]^-$ through an anion-exchange mechanism due to the low solubility of the resulting [Cat][AuX_4] IL.[15] In all discussed examples, the Au recovery yields were high (>90 %), simplifying the hydrometallurgical separation process and significantly reducing the environmental impacts of Au usage.[16] Nevertheless, with some exceptions,[14] the precipitation efficiencies were not determined for conditions similar to that found in PCB leachates, i.e. low ppm levels of Au relative to 100-fold excess of impurities, whilst certain approaches require careful pH adjustment [11,13] or present low selectivity especially in the presence of platinum group metals anions.[17–19].

We serendipitously observed in previous works the unwanted precipitation of the bulky anions $[Ce(NO_3)_6]^{2-}$ and $[Zn(SCN)_4]^{2-}$ upon stoichiometric addition of tetraalkylammonium ($[N_{xxxx}]^+$)-based ILs during liquid–liquid extraction.[20,21] From these observations, we hypothesised that the symmetrical nature of quaternary ammonium salts along with the square planar geometry of $[AuCl_4]^-$ facilitates a specific second-sphere coordination in which $[AuCl_4]^-$ would intercalate between adjacent cations, resulting in its selective precipitation. In this work, the capacity of tetrabutylammonium ($[N_{4444}]^+$)-based salts to selectively recover gold from halide-rich leachates including *aqua regia* is demonstrated both from synthetic and real CPU leachates. Tetrabutylammonium salts are widely used in a numerous applications including as phase transfer catalysts, and are industrially produced ensuring their availability and moderate price.[22] The simple precipitation minimises the excessive use of organic diluents in solvent extraction whilst eliminating the need for complex adsorbent synthesis and post modification, thereby improving the circularity of gold and providing an alternative route to its recovery.

2. Experimental

2.1. Materials

Metal solutions were prepared by dissolution of the following salts from Sigma-Aldrich: gold (III) chloride trihydrate (>99.9 wt%), tin (II) chloride dihydrate (98.0 wt%), platinum (IV) chloride (96.0 wt%). Iron (III) chloride hexahydrate (99.0 wt%) was acquired from Merck whilst nickel (II) chloride hexahydrate (97.0 wt%) and copper (II) chloride dihydrate (98.0 wt%) acquired from BDH Chemicals. Ionic liquid solutions were prepared by dissolution of the respective salts: tetraethylammonium chloride ($[N_{2222}]$Cl; 98.0 wt%) and tetrapropylammonium chloride ($[N_{3333}]$Cl; 98.0 wt%) from Alfa Aesar, tetrabutylammonium nitrate ($[N_{4444}][NO_3]$; 97.0 wt%) and tetrabutylammonium chloride ($[N_{4444}]$Cl; 97.0 wt%) from Sigma-Aldrich, tetrapentylammonium bromide ($[N_{5555}]$Br; 99.0 wt%) from Acros Organics, 1-butyl-1-methylpiperidinium chloride ($[C_4mpip]$Cl; 99.0 wt%) and 1-butyl-3-methylimidazolium chloride ($[C_4mim]$Cl; 99.0 wt%) were supplied by Iolitec. The solvents used throughout were hydrochloric acid (37.0 wt%) from Honeywell, nitric acid (65.0 wt%) from Merck and chloroform (99.0 wt%) from Fisher Scientific. Total X-ray Fluorescence (TXRF) analysis required the use of polyvinyl alcohol (87–90 wt%) and an yttrium standard for ICP (1000 ± 4 mg/L), both from Sigma-Aldrich. All chemicals were used as received without further purification. Ultrapure, double distilled water, passed through a reverse osmosis system and further treated with a Milli-Q plus 185 water purification apparatus, (18.2 MΩ.cm at 25 °C) was used for all experiments.

2.2. Powder X-ray diffraction (PXRD)

PXRD was determined using a Bruker AXS with Cu Kα radiation operating at 45 kV and a spinning discs sample holder. Diffractograms were analysed using the X'pert Highscore Plus software package.

2.3. Single crystal X-ray diffraction (SXRD)

SXRD of the precipitate formed was collected at low temperature (150 K) with monochromated Mo-Kα radiation (λ = 0.71073 Å) on a Bruker Kappa APEX II diffractometer equipped with a CCD area detector. Data reduction was carried out using the SAINT-Plus software package.[23] Multi-scan absorption correction was applied to all intensity data using the SADABS program.[24] The structure was refined via full matrix least squares on F2 using the SHELX-2014 suite.[25] All non-hydrogen atoms were refined with anisotropic thermal parameters. The C—H hydrogen atoms were included in the structure factor calculations in geometrically idealized positions with isotropic thermal displacements depending on the parent atom, using a riding model (1.2 for CH_2 and 1.5 for CH_3). Molecular diagrams were drawn with the Mercury 4.0 software.[26] The Crystal data and selected refinement details are listed in Table S2. The structures were deposited with the Cambridge Crystallographic Data Centre (CCDC).

2.4. Raman spectroscopy

Raman spectra were acquired on a Bruker MultiRAM equipped with a 1064 nm Nd-YAG laser source and a nitrogen cooled germanium detector. All spectra were recorded in the 4000 to 100 cm^{-1} range with a resolution of 4 cm^{-1}. For solid samples, 200 scans and a laser power of 100 mW were used.

2.5. Metal quantification

Metal quantification was performed using a Picofox S2 (Bruker Nano (Billerica, MA, USA)) total reflection X-ray fluorescence spectrometer with a molybdenum X-ray source. The voltage of the X-ray tube was 50 kV and the current 600 μA. All carriers were first pre-treated with 10 μL of silicon in isopropanol solution and dried at 353 K for 30 min. Samples were diluted in 1.0 wt% polyvinyl alcohol acidified at pH = 1.0 using HCl and spiked with a known concentration of YCl_3 to obtain a final standard element concentration of 5 to 20 ppm (depending on the sample metal content). Ten microliters of each solution containing the metals and standard of YCl_3 were added onto a clean carrier and dried on a hot plate at 353 K for 15 min.

2.6. Single element precipitation (metal solutions)

Metal solutions were diluted to 10 ppm (Au, Pt) or 1000 ppm (Cu, Sn, Fe, Ni) using distilled water. Precipitation was carried out by adding the appropriate volume of 0.1 mol/L solution of ionic liquid to the metal solution in a 2 mL centrifuge vial. The vials were stirred in a vortex mixer and allowed to rest for 0.5 to 24 h before centrifuging at 12,000 RPM for 3 min. Supernatant samples were collected before and after precipitation and analysed as described below.

2.7. Treatment of waste printed circuit boards

Printed circuit boards (PCBs) were collected from discarded computers at the University of Aveiro. The collected glass fibre-epoxy substrate CPU (Mobile AMD® Sempron™ 3000 + series, first introduced in 2004) was frozen in liquid nitrogen to facilitate particle size reductions and the detachment of components. Two successive leaching steps were

performed to selectively strip metals from the waste PCB following a previously described protocol.[27] First the shredded waste was leached using 5.0 mol/L nitric acid with a solid to liquid ratio (S/L) of 1:20, at 70 °C for 2 h. Then the residue was dried for 4 h at 100 °C before the second leaching step, using concentrated *aqua regia* in a 1.5:20 S/L ratio, first at 60 °C for 30 min, then 70 °C for another 30 min and finally 80 °C for the remaining 60 min of leaching.

The *aqua regia* leachate was diluted to 10 vol% using distilled water. Precipitation was carried out by adding the appropriate volume of 1.0 mol/L solution of ionic liquid to the diluted leachate in a 50 mL sample tube. The tubes were stirred in a vortex mixer and allowed to rest for 0.5 h before centrifuging at 5000 RPM for 10 min. The supernatant was removed using a syringe. The remaining liquid containing the suspended precipitate was transferred to a small vial to which approximately 1 mL of chloroform was added. After centrifuging, the bottom aqueous phase was removed and the top phase containing the gold and chloroform were left overnight to recover the $[N_{4444}][AuCl_4]$ solid product. Finally, the recrystalized gold precipitate was diluted in 50 vol% ethanol and analysed via TXRF to determine its purity.

2.8. Acidic aqueous biphasic system

The partial AcABS phase diagram of the system composed of $[N_{4444}][NO_3]$ + *aqua regia* (3:1 HCl:HNO_3) + H_2O was determined through the cloud point titration method using a previously described protocol.[21] Briefly, 1 mL of an 80 wt% $[N_{4444}][NO_3]$ were added to a 10 mL temperature-controlled cell kept at 323 K using a water bath (ME-18 V Visco-Thermostat, Julabo with an accuracy of ± 0.1 K). A 50 wt% *aqua regia* solution was added dropwise until the solution became turbid, indicating the formation of a biphasic system. Water was subsequently added dropwise until the system became clear again. These steps are repeated, recording the mass of water and *aqua regia* solution added each time. A system was established as monophasic or biphasic if no change in the cloudiness of the system is observed after 2 mins of vigorous agitation (500 rpm). This threshold was selected to ensure that the initial exothermicity of acid addition did not influence the system properties. The procedure results in a series of mixture points corresponding to the transition between the monophasic and biphasic regions of the phase diagram. All studied system compositions were determined by the weight quantification of all components added within an uncertainty of ± 10^{-3} g using a Mettler Toledo XP205 analytic balance.

3. Results and discussion

3.1. Screening and mechanistic study

A range ammonium salts with varying apolar volume ($[N_{2222}]Cl$ to $[N_{5555}]Br$), planarity ($[C_4mpip]Cl$ *vs* $[N_{4444}]Cl$) and aromaticity ($[C_4mim]Cl$ *vs* $[C_4mpip]Cl$) were tested for their ability to induce gold precipitation. A fixed gold concentration of 10 ppm (0.05 mmol/L), an excess Au:IL ratio of 1:20 (1.0 mmol/L of IL) and an *aqua regia* (3:1 HCl:HNO_3 mixture) concentration of 10 vol% were applied. Under the tested acid condition, $[AuCl_4]^-$ is expected to be the sole gold complex in solution.[28] The precipitation yields were calculated according to Eq. (1), with the results presented in Fig. 1**A** along with the generic structure of each salt family.

$$Precipitation\ Yield = 1 - \frac{[Au]_{final}}{[Au]_{initial}} \quad (1)$$

where the subscript final and initial indicate the sampling time.

From Fig. 1**A**, the $[C_4mpip]Cl$ and $[C_4mim]Cl$ ILs displayed little to no ability to induce Au precipitation contrary to that reported for the equivalent system with octyl alkyl chains.[15] Interestingly for the symmetrical $[N_{xxxx}]^+$ salts, no significant precipitation was observed until × ≥ 4, resulting in a maximum 92.6 ± 0.1 % Au precipitation in only 0.5 h using $[N_{4444}][NO_3]$. Further increase in the alkyl chain length or nature of the initial IL anion does not significantly influence the precipitation yield. In addition to the salts mentioned above, the tertiary amine precursor to the $[N_{4444}]^+$ cation, tributylamine, was also tested due to it's potential protonation under the acidic conditions tested. However, only 33.4 ± 5.2 % of Au precipitation under the same conditions as in Fig. 1**A** was obtained, demonstrating the importance of the $[N_{4444}]^+$ cation. The absence of functional groups in $[N_{xxxx}]Cl$ salts entails a lack of directional interactions with $[AuCl_4]^-$, relying only on diffuse electrostatic and van der Waals forces. As such, the precipitation yield depends on the (i) energetic penalty to ion dehydration, estimated using the Gibbs energy of hydration ($\Delta_{Hyd}G^0$), and (ii) the formation of apolar cavities capable of accommodating $[AuCl_4]^-$, which is dependent on the radius of $[N_{xxxx}]^+$ (r_{vdW}). These properties as a function of the $[N_{xxxx}]^+$ alkyl chain length (x = 1–4) are summarised in Fig. 1**B**. When considering that the terminal carbon atoms of two neighbouring alkyl chains make up the vertices of a partial apolar cavity, schematically illustrated in Fig. 1**B**, only for x ≥ 4 is $[N_{xxxx}]^+$ able to fully envelop the $[AuCl_4]^-$ thereby ensuring the complete exclusion of water molecules (thermochemical diameter = 5.76 Å).[29] This size-dependent criteria is compounded by the increase in $\Delta_{Hyd}G^o$ of $[N_{xxxx}]^+$ with increasing ×, facilitating the formation of ion-pairs in solution with $[AuCl_4]^-$ as qualitatively suggested by the Hofmeister series.

To gain further insight into the nature of the precipitate, the same experiment as in Fig. 1**A** was repeated with $[N_{4444}][NO_3]$ using a 100x more concentrated system ([Au] = 1000 ppm). The resulting amorphous solid was recrystallised in $CHCl_3$ under slow evaporation to yield crystals suitable single crystal X-ray analysis (SCXRD). The crystal structure is presented in Fig. 2 and a summary of the crystal data and relevant refinement parameters are given in Table S2. The $[AuCl_4]^-$ anion positions itself parallel to one $[N_{4444}]^+$ butyl chain with the central gold atom nearer to the carbon atoms than the cationic nitrogen. In addition to weak electrostatic contributions (shortest *N*-Cl = 4.609 Å), van der Waal and non-classical C—H•••Cl hydrogen-bonding interactions

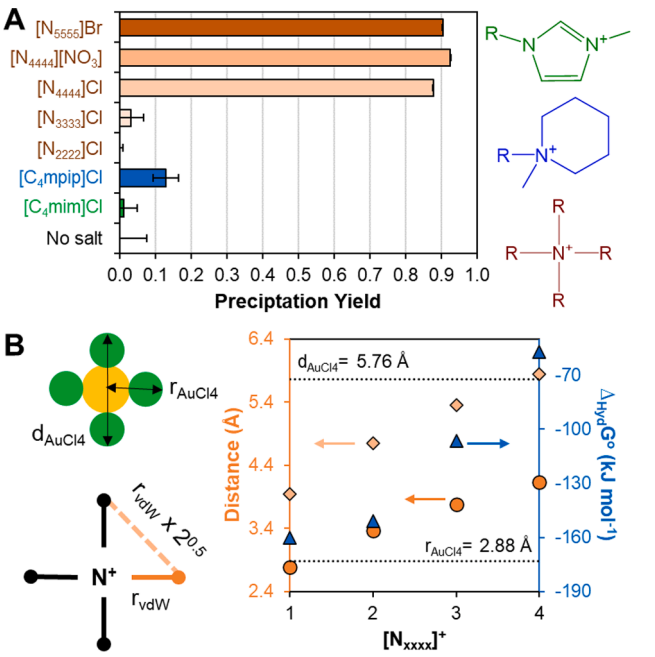

Fig. 1. A) Gold precipitation yield after 0.5 h using different ammonium salts along with their generic structure ([Au] = 10 ppm; Au:Salt = 1:20, 10 vol% *aqua regia*). B) Properties of isolated tetraalkylammonium cations ($[N_{xxxx}]^+$) as a function of the alkyl chain length including the van der Waals radii (r_{vdW}) and the standard Gibbs energy of hydration ($\Delta_{Hyd}G^o$). The radius of $[AuCl_4]^-$ was obtained from ref [29], all $[N_{xxxx}]^+$ properties were taken from ref [30] and are available in Table S1 of the ESI.

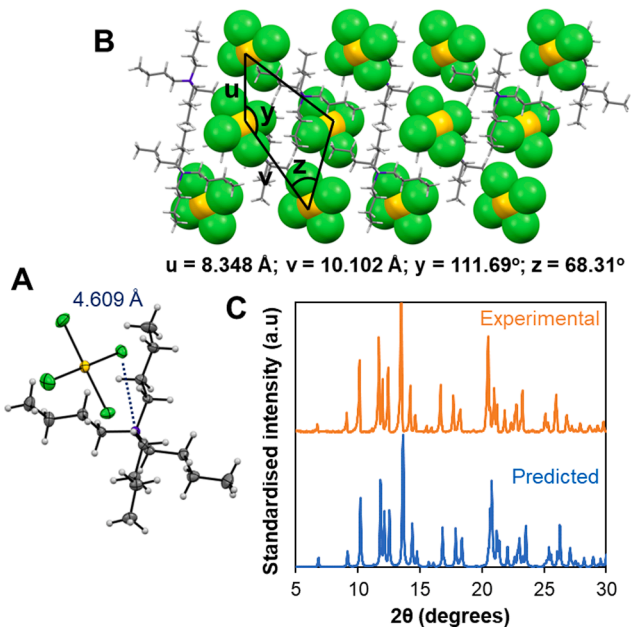

Fig. 2. A) X-ray crystal structure of $[N_{4444}][AuCl_4]$ with thermal ellipsoids (50 % probability level) and showing the shortest *N*-Cl bond. Atom colours: blue = N; grey = C; white = H, green = Cl; yellow = Au. B) crystal packing of $[N_{4444}][AuCl_4]$ along the b-axis. C) Comparison of the predicted powder X-ray diffraction from single crystal structure with that experimentally obtained. (For interpretation of the references to colour in this figure legend, the reader is referred to the web version of this article.)

(C—H•••Cl ranging from 2.790 to 2.946 Å) appear to stabilise the precipitate similarly to that reported for diamides.[14] The $[N_{4444}]^+$ cations arrange themselves in an infinite supramolecular chain with each adopting a trans configuration as shown in Fig. 2**B**; the torsion angles are listed in Table 1. As hypothesised in Fig. 1**B**, each $[AuCl_4]^-$ is at the centre of a rhombohedral cavity made of 8 butyl chains from 4 $[N_{4444}]^+$ cations, effectively encapsulating the former.

To confirm if the superstructure presented in Fig. 2**B** is representative of the bulk precipitate nanostructure, the experimental powder XRD (PXRD) of the bulk precipitate is compared with the simulated patterns based on the SCXRD data and shown in Fig. 2**C**. The excellent agreement between both validates the ordered nature of the precipitate. Comparison of the Raman spectra for the solid $[N_{4444}][NO_3]$ precursor with the bulk precipitate in **Figure S1** shows the complete disappearance of the nitrate counter-anion band at 1030 cm^{-1} and the appearance of bands in the lower wavenumber region at 168, 324, and 347 cm^{-1} characteristic of anionic chloro complexes,[31] suggesting a quantitative anion-exchange between $[NO_3]^-$ and $[AuCl_4]^-$. This observation along with the results in Fig. 1**A** indicate that the counter-anion of $[N_{4444}]^+$ has a negligible influence on the Au recovery yield as long as it can be readily exchanged with $[AuCl_4]^-$. The likelihood of complete anion-exchange is given by the cation–anion interaction energy which approximately follows the Hofmeister series, and proceeds in decreasing order of anion-exchange as $[AuX_4]^-$ (X = Cl/Br/I) > $[HSO_4]^-$ > I^- > $[NO_3]^-$ > Br^- > $[CH_3COO]^-$ > Cl^-.[32,33] Although a nitrate-based IL was here selected, it was solely done to match one of the main anions in *aqua regia* solutions as Au precipitation entails the formation of new IL complex of $[N_{4444}][AuCl_4]$, allowing to potentially substitute the nitrate anion by a more economical alternative.

3.2. Optimisation of gold precipitation

As the best performing precipitating agent, $[N_{4444}][NO_3]$ was selected for gold recovery and the process optimised as function of Au:IL ratio, time, *aqua regia* concentration, and temperature. Unless otherwise specified, standard conditions of [Au] = 10 ppm, Au:IL = 1:20, [*aqua regia*] = 10 vol% and t = 0.5 h were applied. The results are presented in Fig. 3**A-B** and in Figure S2. From the precipitation stoichiometry given in Eq. (2), a 1:1 ratio of Au(III) to IL is theoretically sufficient to induce precipitation.

$$[N_{4444}]^+_{aq} + NO^-_{3,aq} + HAuCl_{4,aq} \leftrightarrow [N_{4444}][AuCl_4]_s + HNO_{3,aq} \quad (2)$$

However, gold precipitation was found to occur in excess IL to Au ratios, with the precipitation efficiency increasing both with time and amount of IL used, albeit with diminishing returns after a certain point as shown in Fig. 3**A**. Au precipitation increases linearly with the amount of IL used until an excess Au:IL of 1:20, after which a plateau is reached. Over 92 % of Au precipitates when using Au:IL of 1:20, reaching a maximum of 97.9 % for Au:IL ≥ 1:50. For Au:IL < 1:10, a moderate dependency with precipitation time is observed which disappears for greater IL:Au ratios as shown in the inset of Fig. 3**A**. The observation that gold recovery requires a greater than stoichiometric concentration of ligand suggests that its precipitation is dictated by adsorption onto the $[N_{4444}]^+$ alkyl chains and subsequent nucleation. From the results in Fig. 3**A**, the solubility product of $[N_{4444}][AuCl_4]$ (K_{Au}) was determined as 5.57 ± 1.76x10^{-9} mol^2 L^{-2} as per Eq. (3).

$$K_{Au} = [N_{4444}]^+_{aq,final} \times [AuCl_4]^-_{aq,final} \quad (3)$$

The precipitation yield decreased for *aqua regia* concentrations superior to 20 vol% as indicated in Fig. 3**B**, suggesting the suitability of this approach for $[H^+]$ concentrations below 3.2 mol/L. However, it is unclear if this concentration threshold obtained in *aqua regia* is directly transposable to other acid solutions such as HCl. In contrast to Au precipitation using amides, which is protonation dependent and therefore increases with acid concentration,[12–14] an inverse tendency was observed for the permanently charged ammonium. A possible explanation could be that by increasing the acid concentration, the reaction in Eq. (2) is driven towards the reactant side according to Le Chatelier's principle, lowering the precipitation yield. It is worth noting that *aqua regia* dilution and amount of IL used might not be independent from each other. Platinum was shown to precipitate when using imidazolium-based ILs in 1:1 and 1:2 Pt:IL ratios with yields of 84 to 98 % but only when Cl^- concentrations are approximately 1.0 mol/L. Precipitation was completely inhibited in a 11.0 mol/L HCl solution.[19] Finally, temperature was found to have little influence on the precipitation yield as shown in Figure S2, with a small decrease observed from 92.6 % at 23 °C to 86.9 % at 50 °C.

The selectivity of Au towards representative metals found in PCB leachate, namely Cu(II), Ni(II), Fe(III), Sn(II), and Pt(IV), was determined based on mono-elemental precipitation essays at 10 vol% *aqua regia*. A concentration of 1000 ppm and ratio of metal:IL of 1:5 was used for all metals except Pt for which a concentration of 10 ppm and Pt:IL of

Table 1
Selected torsion angles of the $[N_{4444}]^+$ in the single crystal structure of $[N_{4444}][AuCl_4]$ and $[N_{4444}]_2[PtCl_6]$. Each C—C—C—C corresponds to the torsion of one butyl chain whilst C—C—N—C where measure for symmetrical alkyl chains relative to the central nitrogen atom.

Torsion angle (degrees)	$[N_{4444}][AuCl_4]$				$[N_{4444}]_2[PtCl_6]$			
	1	2	3	4	1	2	3	4
C—C—C—C	178.86	177.17	176.23	177.41	179.39	176.94	69.13	170.49
C—C—N—C	175.85	177.70	–	–	167.35	37.28	–	–

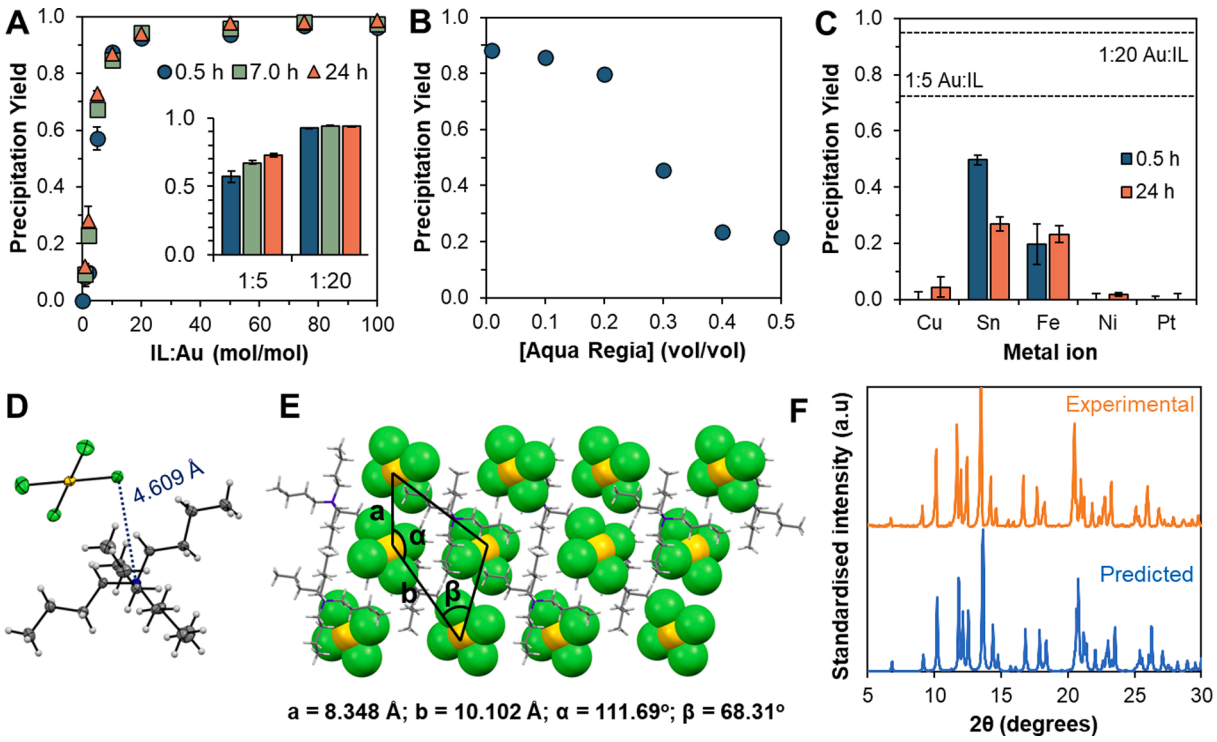

Fig. 3. Gold precipitation as a function of the A) Au to $[N_{4444}][NO_3]$ ratio and time as well as B) the *Aqua regia* concentration. Unless otherwise specified, standard conditions of [Au] = 10 ppm, Au:IL = 1:20, [*Aqua Regia*] = 10 vol% and t = 0.5 h were applied. C) Precipitation yields of Cu(II), Sn(II), Fe(III), Ni(II), and Pt(IV) from mono-elemental solutions in 10 vol% *aqua regia* after 0.5 and 24 h. A concentration of 1000 ppm and ratio of metal:IL of 1:5 was used for all metals except Pt for which a concentration of 10 ppm and Pt:IL of 1:20 was applied.

1:20 was applied. The 1:5 ratio was used to achieve a lower reagent use. Based off the gold tests, this ratio is sufficient to induce precipitation if it were to occur. Aqueous phase concentrations were measured 0.5 and 24 h after $[N_{4444}][NO_3]$ addition, with the results presented in Fig. 3C. The precipitation of gold is highly selective against Cu, Ni, and Pt under the tested conditions, with negligible precipitation of these metals observed within experimental error. In contrast, 26.9 % and 23.3 % of Sn and Fe were recovered after 24 h although the unexpected trend in Sn precipitation with time indicates that some portion is due to its hydrolysis. [34,35] Results suggest that metal recovery is not entirely dependent on the formation of anionic chlorometalate complexes (tetrahedral $FeCl_4^-$ and $SnCl_4^{2-}$) as no precipitation was observed for Pt despite the prevalence of the homoleptic $PtCl_6^{2-}$ at the studied chloride concentration. [36] After one week of contact, a crystalline solid appeared on the wall of the

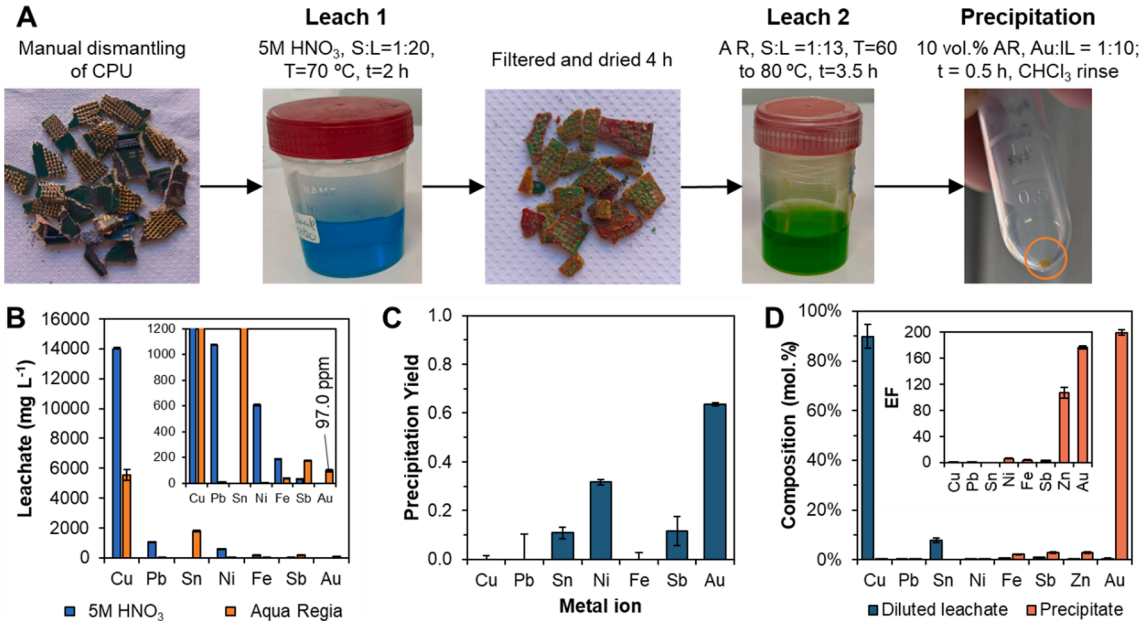

Fig. 4. A) Main steps applied along with their respective experimental conditions for the recovery of Au from waste CPUs. B) Compositions of the leach 1 and 2 solutions. C) Metal precipitation yields from the diluted *aqua regia* (AR) leachate (10 vol%) for an Au:IL ratio of 10 and t = 0.5 h. D) Comparison between the metallic content of the leachate and the precipitate after $CHCl_3$ rinse in molar percentage. Inset: Enrichment factor (EF) of the final precipitate.

Pt solution which was analysed by SCXRD, Figure S3, indicating the formation of $[N_{4444}]_2[PtCl_6]$. Notably, the greater volume of the octahedral $[PtCl_6]$ forces a change in the preferred arrangement of one cationic butyl chain from trans to gauche whilst a C—C—N—C dihedral has a value of 37.3° resulting in a sterically unfavourable configuration (see Table 1 for torsion angles). This greater energetic barrier to crystallisation can be exploited for the kinetically based separation of Au from Pt and emphasises that the precipitate chemical structure influences the selectivity.

3.3. Application towards Au recovery from waste CPU

As a proof-of-concept, the recovery of gold from real waste CPU leachate was attempted. To this end, two successive leaching stages were performed to selectively strip metals from waste CPU (Mobile AMD® Sempron™ 3000 + series) following a previously described protocol.[27] The process is summarised in Fig. 4**A** and the composition of the first and second leachate using 5.0 mol L^{-1} HNO_3 and concentrated *aqua regia* respectively is given in Fig. 4**B**. The use of a preliminary nitric acid leach yields a purified Cu leachate (92.0 mol.%) with lesser amount of Ni (4.3 mol.%), Pb (2.2 mol.%), and trace quantities of Fe and other metals with no loss of Au. Treatment of this leachate is beyond the scope of this work and can be achieved using reported techniques such as the selective precipitation of Pb[37] or the solvent extraction separation of Cu from Ni.[38] A gold concentration of 97.0 ppm ($49x10^{-4}$ mol L^{-1}) was obtained in the concentrated *aqua regia* leachate – representing only 0.47 mol.% of the metallic content in solution with Cu (83.2 mol.%) and Sn (14.2 mol.%) being the major impurities. The concentrated leachate was diluted as to obtain a 10 vol% *aqua regia* solution. To account for the complexity of the real leachate, small scale tests were conducted to confirm the previously mentioned experimental conditions are appropriate to application in the real sample, with Au:IL ratios of 1:5 to 1:20 and precipitation times of 0.5 to 24 h tested. Two metrics were considered to evaluate the selectivity of the metal separation: the gold percentage in the metallic content of the precipitate and its ratio with the percentage of gold in the leachate – the enrichment factor (EF), as defined in Eq. (4).

$$EF = \frac{mol\%(Au)_{precipitate}}{mol\%(Au)_{leachate}} \quad (4)$$

The results are presented in Figures S4 and S5 and confirm that the optimal selective conditions are consistent with those from single element essays, namely a Au:IL ratio of 1:10 and t = 0.5 h. The greater purity is achieved at the expense of a lower overall gold precipitation compared to using 1:20 Au:IL – 70 % versus 90 %. Importantly, dilution of the leachate to 10 vol% induced the precipitation of some of the harder cations, namely Sn and Sb, after 72 h even in the absence of $[N_{4444}][NO_3]$ as shown in Figure S6. As previously mentioned, this could be assigned to hydrolysis of the harder metal ions which is further exacerbated by the precipitation of the partially dissolved epoxy resin from the printed circuit board. The latter was confirmed by FTIR analysis (not shown) of the precipitate recovered for dilutions below 10 vol% *aqua regia* which presented a number of CH_2 and CH_3 bands between 2900 and 3000 cm^{-1}. Unwanted co-precipitation could be mitigated by using a shorter precipitation time of 0.5 h.

Applying these parameters to a larger volume of diluted leachate (50 mL) resulted in the observable formation of light-yellow precipitate. Metal analysis of the liquid phase shown in Fig. 4**C** indicates no precipitation for copper and about 10 % for Sn, while managing 64 % Au precipitation yield. The composition of the precipitate was calculated through mass balance to be 14.7 mol.% Au and 76.3 mol.% Sn, the remainder being Sb and Ni impurities. However, the far greater amount of precipitated Sn relative to the initial $[N_{4444}][NO_3]$ concentration suggests that it primarily co-precipitate due to hydrolysis and not as the tetrabutylammonium salt. As such, the recovered solid was contacted with a minimal quantity of $CHCl_3$ and filtered with the aim of selectively dissolving the organic chloroaurate salts. The $CHCl_3$ filtrate was evaporated to yield a golden salt shown in Fig. 4**A**. Metal analysis of the final solid indicates a significantly improved gold concentration of 91.4 mol. %, shown in Fig. 4**D** and listed in Table S3. The final Au concentration along with the associated EF of 177 confirms the selectivity of $[N_{4444}]^+$ as precipitant towards Au. No Au could be quantified in the residual solid following the $CHCl_3$ washing stage, demonstrating the absence of Au losses at this stage. Although $CHCl_3$ is not regarded as a green solvent, the small quantity of obtained precipitate (~1 mg) precluded the identification of a more benign alternative. However, existing solubility results on the comparable $[N_{8888}][AuCl_4]$ hints at the potential substitution of $CHCl_3$ by the more biocompatible methanol.[39] The recovered gold precipitate can be reduced using a reductant such as sodium metabisulfite ($Na_2S_2O_5$) after resuspension.

Whilst the reported gold recovery yield and purity from simple acidic solutions compares favorably with that obtained using functionalized adsorbents[40,41] or by solvent extraction (>90 %),[42–44] further work is required to (i) reduce the required the IL:Au ratio and (ii) improve the precipitation efficiency of 64 % from real CPU leachates. A comparable gold precipitation yield was of 70 % was achieved using diamide precipitating agents in the presence of 29 metal ions with excellent selectivity in 2.0 mol/L HCl.[14] However, the more problematic Sn and Sb ions were not included in this screening. Nevertheless, the final purity of the precipitate from a real matrix obtained herein is encouraging when considering the simplicity of precipitation process against the complexity of the real leachate, whilst avoiding the need for large volumes of organic solvent inherent to liquid–liquid extraction or the synthesis of sophisticated materials. Due to the low concentration of $[N_{4444}][NO_3]$ used of 1.0 mmol/L (0.3 g/L) in this study, no attempts at ligand recovery and regeneration was made although various options for ionic liquid recovery exist including membrane separation, crystallization or by solvent extraction.[45] Considering the average gold price in 2022 of approximately 51 000 € kg^{-1} [46] and the bulk price range of hydrophilic tetrabutylammonium-based salt from 20 to 200 € kg^{-1},[47] depending on the counter-anion selection, the recovery process appears as economical.

3.4. Alternative Au recovery using an acidic aqueous biphasic system (AcABS)

As an alternative to the selective precipitation of Au using $[N_{4444}][NO_3]$, the same quaternary ammonium salt was investigated as a phase-former in an AcABS relying on the *aqua regia* leachate as salting-out agent. This allows to compare the selectivity of the precipitation approach versus liquid–liquid separation and provide an alternative to precipitation for higher acid concentration where the recovery yield decreases. AcABS uses the inorganic acid content of concentrated leachates to drive the reversible phase transition from monophasic to biphasic of a hydrophilic quaternary ammonium IL, thereby substituting the inorganic salt in traditional aqueous biphasic systems (ABS).[21,48] The acid driven phase transition of AcABS from a mono- to biphasic system overcomes the traditional instability of ABS at low pH values whilst retaining their advantageous qualities, including the use of water as the main component of the system, the absence volatile organic diluents and a decreased phase viscosity resulting in faster mass transfer. The partial AcABS phase diagram of the system composed of $[N_{4444}][NO_3]$ + *aqua regia* was determined through the cloud point titration method at two different temperatures and is presented in Fig. 5**A**. The experimental binodal points are provided in Table S4.

Following leaching of the CPU as per the protocol presented in Fig. 4**A**, AcABS mixtures containing approximately 16 wt% *aqua regia* leachate and 20 wt% $[N_{4444}][NO_3]$ were prepared and placed in a 323 K oven. After phase separation, samples were collected from each phase for metal quantification. In this case, the large excess of $[N_{4444}][NO_3]$ and the resulting change in the polarity of the IL-rich phase upon phase

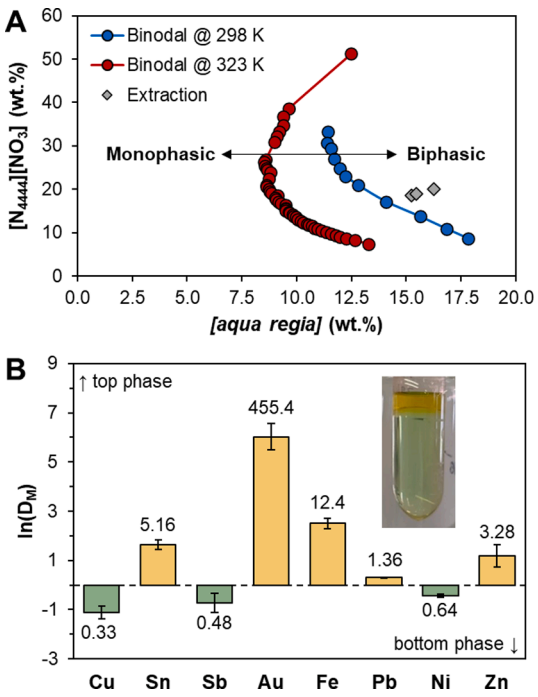

Fig. 5. A) AcABS phase diagram of the $[N_{4444}]NO_3$ + *aqua regia* + water ternary system at 298 and 323 K along with the mixture point compositions used for the liquid–liquid extraction tests. The experimental binodal points are provided in Table S4. B) Distribution coefficients of the major elements found in the *aqua regia* leachate in the AcABS system of $[N_{4444}][NO_3]$ + *aqua regia* + water at 323 K. An AcABS composition of 20 wt% IL and ~ 16 wt% *aqua regia* was used. Inset: Appearance of the AcABS at equilibrium with the IL-rich phase on top.

separation could effectively solvate the resulting $[N_{4444}][AuCl_4]$ extract, with no precipitation observed. Distribution coefficients for each major metal present in the leachate (D_M) were calculated using equation (5) to quantify the preferential partition of each metal. The resulting D_M values are shown in Fig. 5**B** and summarised in Table 2.

$$D_M = \frac{[M]_{IL-richphase}}{[M]_{Acid-richphase}} \quad (5)$$

where [M] is the concentration of metal M and the subscript IL-rich and acid-rich indicate the respective phase. Although only one mixture point was investigated, $[N_{4444}][NO_3]$ retains its affinity for $[AuCl_4]^-$ when used in an AcABS as demonstrated by the quantitative gold extraction ($D_{Au} > 100$). The selectivity of the AcABS separation towards Au for a given metal M was determined by calculating the separation factor (SF) as per equation (6), with the values presented in Table 2.

$$SF_{Au/M} = \frac{D_{Au}}{D_M} \quad (6)$$

To compare the obtained selectivity of AcABS against the precipitation approach for a given metal (M) present in the leachate, the ratio of the EF_{Au} to EF_M were calculated for the precipitate in a manner akin to the $SF_{Au/M}$ and are available in Table 2. The two separation techniques present a comparable selectivity, with the SF and EF ratios in the same order of magnitude for most metals, confirming AcABS as a potential alternative to precipitation for higher *aqua regia* concentrations not compatible with the latter. However, the precipitation method achieved a greater relative selectivity for the separation of Au from Cu and Sn, the two main impurities present in the PCB leachate with Sn being absent from the precipitate altogether. The same IL can therefore be used either as a precipitant or as an AcABS phase-former depending on the acid concentration, providing further flexibility to the recovery process.

Table 2
Distribution coefficients of the major elements found in the CPU leachate in the AcABS system of $[N_{4444}][NO_3]$ + *aqua regia* + water at 323 K and the derived gold separation factors (SF). These are compared against the enrichment factor (EF) achieved using the precipitation approach (N.D. – not detected in the solid phase).

Element	D_M	$SF_{Au/M}$	EF_M	EF_{Au} / EF_M
Fe	12.4 ± 2.56	38.8 ± 21.2	3.49 ± 0.41	51.0 ± 5.4
Ni	0.64 ± 0.04	866 ± 256	5.80 ± 0.61	30.7 ± 2.9
Cu	0.33 ± 0.09	1311 ± 345	0.003 ± 0.00	≫ 1000
Zn	3.53 ± 1.68	158 ± 101	107 ± 8.57	1.66 ± 0.11
Sn	5.22 ± 0.99	91.9 ± 51.5	N.D.	≫ 1000
Sb	0.51 ± 0.19	1021 ± 590	2.88 ± 0.28	61.7 ± 5.2
Au	455 ± 231	–	177 ± 2.03	–
Pb	1.36 ± 0.01	335 ± 171	0.48 ± 0.00	365 ± 3.3

4. Conclusions

The results herein provide a simple and mild alternative to gold recycling using reduced consumption of reagent. The $[N_{4444}]^+$ cation was proven to be a selective precipitant for Au under a variety of conditions including mildly acidic concentrations compatible with *aqua regia* leachates. The precipitation yield was dependent on the Au:IL ratio, the acid concentration, and the structures of the precipitates. The high selectivity towards Au relative to Cu, Ni, or Pt allows the disclosed methodology to be applied to a range of relevant and/or difficult separations. The pertinence of this approach was demonstrated on real CPU leach solution with a final gold precipitate of 91.4 mol.% recovered with 64 % efficiency. Comparison of the $[N_{4444}][NO_3]$ selectivity when applied as a precipitating agent or as an extractant in AcABS indicate that the IL retains its affinity for gold independent of its application. This provided further flexibility to the recovery process as it can be tailored to the aqueous phase acidity. Future work must address the valorisation the $[N_{4444}][AuCl_4]$ precipitate and the recovery of the precipitating reagent. Of particular interest is the possibility to extend this approach to the separation of the square planar $[AuCl_4]^-$ from the solutions of platinum group metals as well as to other gold-bearing solutions in which anionic auro complexes are present.

CRediT authorship contribution statement

André F.M. Nogueira: Investigation, Writing – original draft, Writing – review & editing. **Ana R.F. Carreira:** Investigation, Writing – review & editing. **Sílvia J.R. Vargas:** Investigation, Writing – review & editing. **Helena Passos:** Supervision, Conceptualization, Writing – review & editing. **Nicolas Schaeffer:** Writing – original draft, Supervision, Conceptualization, Writing – review & editing. **João A.P. Coutinho:** Funding acquisition, Writing – review & editing.

Declaration of Competing Interest

The authors declare that they have no known competing financial interests or personal relationships that could have appeared to influence the work reported in this paper.

Data availability

Data will be made available on request.

Acknowledgments

The authors would like to thank Dr. Paula Brandão and Maria C.C. Azevedo for help with the SCXRD and Raman data acquisition, respectively. This work was developed within the scope of the project CICECO-Aveiro Institute of Materials, UIDB/50011/2020, UIDP/50011/2020 & LA/P/0006/2020, financed by national funds through the FCT/MEC

(PIDDAC). H. Passos and A.R.F. Carreira acknowledge FCT, under the Scientific Employment Stimulus Individual Call (CEECIND/00831/2017) and Ph.D. grants SFRH/BD/143612/2019, respectively. N. Schaeffer acknowledges the national funds (OE), through FCT in the scope of the framework contract foreseen in the numbers 4, 5 and 6 of the article 23, of the Decree-Law 57/2016, of August 29, changed by Law 57/2017, of July 19.

Data availability

Data will be made available on request.

Appendix A. Supplementary material

Includes: X-ray crystal structure of $[N_{4444}]_2[PtCl_6]$; SCXRD data and refinement parameters; Raman characterisation of the $[N_{4444}][AuCl_4]$ precipitate; Gold precipitation yield optimisation from waste CPU *aqua regia* leach solutions; Experimental AcABS binodal compositions. Supplementary data to this article can be found online at https://doi.org/10.1016/j.seppur.2023.123797.

References

[1] G.J. Hutchings, M. Brust, H. Schmidbaur, Gold—an introductory perspective, Chem. Soc. Rev. 37 (2008) 1759–1765, https://doi.org/10.1039/B810747P.
[2] J. Cui, L. Zhang, Metallurgical recovery of metals from electronic waste: a review, J. Hazard. Mater. 158 (2008) 228–256, https://doi.org/10.1016/j.jhazmat.2008.02.001.
[3] S. Adrian, M.B. Drisse, Y. Cheng, L. Devia, O. Deubzer, F. Goldizen, J. Gorman, S. Herat, S. Honda, G. Iattoni, W. Jingwei, L. Jinhui, D.S. Khetriwal, J. Linnell, F. Magalini, I.C. Nnorom, P. Onianwa, D. Ott, A. Ramola, U. Silva, R. Stillhart, D. Tillekeratne, V. Van Straalen, M. Wagner, T. Yamamoto, X. Zeng, The Global E-waste Monitor 2020: Quantities, flows, and the circular economy potential, Bonn/Geneva/Rotterdam, 2020.
[4] M.R. Bilesan, I. Makarova, B. Wickman, E. Repo, Efficient separation of precious metals from computer waste printed circuit boards by hydrocyclone and dilution-gravity methods, J. Clean. Prod. 286 (2021), 125505, https://doi.org/10.1016/J.JCLEPRO.2020.125505.
[5] M.D. Rao, K.K. Singh, C.A. Morrison, J.B. Love, Challenges and opportunities in the recovery of gold from electronic waste, RSC Adv. 10 (2020) 4300–4309, https://doi.org/10.1039/C9RA07607G.
[6] H. Wu, L.O. Jones, Y. Wang, D. Shen, Z. Liu, L. Zhang, K. Cai, Y. Jiao, C.L. Stern, G. C. Schatz, J.F. Stoddart, High-efficiency gold recovery using Cucurbit[6]uril, ACS Appl. Mater. Interfaces. 12 (2020) 38768–38777, https://doi.org/10.1021/ACSAMI.0C09673.
[7] D. Purchase, G. Abbasi, L. Bisschop, D. Chatterjee, C. Ekberg, M. Ermolin, P. Fedotov, H. Garelick, K. Isimekhai, N.G. Kandile, M. Lundström, A. Matharu, B. W. Miller, A. Pineda, O.E. Popoola, T. Retegan, H. Ruedel, A. Serpe, Y. Sheva, K. R. Surati, F. Walsh, B.P. Wilson, M.H. Wong, Global occurrence, chemical properties, and ecological impacts of e-wastes (IUPAC Technical Report), Pure Appl. Chem. 92 (2020) 1733–1767, https://doi.org/10.1515/PAC-2019-0502.
[8] C.A. Fleming, Hydrometallurgy of precious metals recovery, Hydrometallurgy 30 (1992) 127–162, https://doi.org/10.1016/0304-386X(92)90081-A.
[9] G. Senanayake, Gold leaching in non-cyanide lixiviant systems: critical issues on fundamentals and applications, Miner. Eng. 17 (2004) 785–801, https://doi.org/10.1016/J.MINENG.2004.01.008.
[10] Z. Liu, A. Samanta, J. Lei, J. Sun, Y. Wang, J.F. Stoddart, Cation-dependent gold recovery with α-Cyclodextrin facilitated by second-sphere coordination, J. Am. Chem. Soc. 138 (2016) 11643–11653, https://doi.org/10.1021/JACS.6B04986.
[11] Z. Liu, M. Frasconi, J. Lei, Z.J. Brown, Z. Zhu, D. Cao, J. Iehl, G. Liu, A. C. Fahrenbach, Y.Y. Botros, O.K. Farha, J.T. Hupp, C.A. Mirkin, J.F. Stoddart, Selective isolation of gold facilitated by second-sphere coordination with α-cyclodextrin, Nat. Commun. 41 (4) (2013) 1–9, https://doi.org/10.1038/ncomms2891.
[12] C.C. Shaffer, W. Liu, A.G. Oliver, B.D. Smith, Supramolecular paradigm for capture and Co-Precipitation of Gold(III) Coordination Complexes, Chem. – A Eur. J. 27 (2021) 751–757, https://doi.org/10.1002/CHEM.202003680.
[13] A. Nag, M.R. Islam, T. Pradeep, Selective extraction of gold by niacin, ACS Sustain. Chem. Eng. 9 (2021) 2129–2135, https://doi.org/10.1021/ACSSUSCHEMENG.0C07409.
[14] L.M.M. Kinsman, B.T. Ngwenya, C.A. Morrison, J.B. Love, Tuneable separation of gold by selective precipitation using a simple and recyclable diamide, Nat. Commun. 121 (12) (2021) 1–8, https://doi.org/10.1038/s41467-021-26563-7.
[15] N. Papaiconomou, G. Vite, N. Goujon, J.M. Lévêque, I. Billard, Efficient removal of gold complexes from water by precipitation or liquid–liquid extraction using ionic liquids, Green Chem. 14 (2012) 2050–2056, https://doi.org/10.1039/C2GC35222B.
[16] P. Pati, S. McGinnis, P.J. Vikesland, Waste not want not: life cycle implications of gold recovery and recycling from nanowaste, Environ. Sci. Nano. 3 (2016) 1133–1143, https://doi.org/10.1039/C6EN00181E.
[17] W. Liu, A.G. Oliver, B.D. Smith, Macrocyclic receptor for precious gold, platinum, or palladium coordination complexes, J. Am. Chem. Soc. 140 (2018) 6810–6813, https://doi.org/10.1021/JACS.8B04155.
[18] H. Wu, Y. Wang, L.O. Jones, W. Liu, L. Zhang, B. Song, X.Y. Chen, C.L. Stern, G. C. Schatz, J.F. Stoddart, Selective Separation of Hexachloroplatinate(IV) Dianions Based on Exo-Binding with Cucurbit[6]uril, Angew. Chemie Int. Ed. 60 (2021) 17587–17594, https://doi.org/10.1002/ANIE.202104646.
[19] S. Génand-Pinaz, N. Papaiconomou, J.M. Leveque, Removal of platinum from water by precipitation or liquid–liquid extraction and separation from gold using ionic liquids, Green Chem. 15 (2013) 2493–2501, https://doi.org/10.1039/C3GC40557E.
[20] H. Passos, B. Cruz, N. Schaeffer, C. Patinha, E.F. Da Silva, J.A.P. Coutinho, Selective sequential recovery of zinc and copper from acid mine drainage, ACS Sustain. Chem. Eng. 9 (2021) 3647–3657, https://doi.org/10.1021/ACSSUSCHEMENG.0C07549.
[21] N. Schaeffer, S.J.R. Vargas, H. Passos, P. Brandão, H.I.S. Nogueira, L. Svecova Papaiconomou, J.A.P. Coutinho, A HNO3-responsive aqueous biphasic system for metal separation: application towards Ce(IV) Recovery, ChemSusChem. 14 (14) (2021) 3018–3026, https://doi.org/10.1002/CSSC.202101149.
[22] B.K. Banik, B. Banerjee, G. Kaur, S. Saroch, R. Kumar, Tetrabutylammonium Bromide (TBAB) Catalyzed Synthesis of Bioactive Heterocycles, Molecules 25 (24) (2021) 5918, https://doi.org/10.3390/MOLECULES25245918.
[23] Bruker SAINT-plus Bruker AXS Inc.,Madison, Wisconsin, USA, 2007, (n.d.), (n.d.).
[24] G.M. Sheldrick, SADABS, program for empirical absorption correction of area detector data, University of Gottingen, Gottingen, Germany., (n.d.), 2010.
[25] Sheldrick, G.M., SHELX Version 2014/7, (n.d.)., (n.d.).
[26] C.F. MacRae, I. Sovago, S.J. Cottrell, P.T.A. Galek, P. McCabe, E. Pidcock, M. Platings, G.P. Shields, J.S. Stevens, M. Towler, P.A. Wood, Mercury 4.0: from visualization to analysis, design and prediction, J. Appl. Crystallogr. 53 (2020) 226–235, https://doi.org/10.1107/S1600576719014092.
[27] M.C. Hespanhol, B.M. Fontoura, J.C. Quintão, L.H.M. da Silva, Extraction and purification of gold from raw acidic electronic leachate using an aqueous biphasic system, J. Taiwan Inst. Chem. Eng. 115 (2020) 218–222, https://doi.org/10.1016/J.JTICE.2020.10.027.
[28] A. Usher, D.C. McPhail, J. Brugger, A spectrophotometric study of aqueous Au(III) halide–hydroxide complexes at 25–80 °C, Geochim. Cosmochim. Acta. 73 (2009) 3359–3380, https://doi.org/10.1016/J.GCA.2009.01.036.
[29] M.C. Simoes, K.J. Hughes, D.B. Ingham, L. Ma, M. Pourkashanian, Estimation of the thermochemical radii and ionic volumes of complex Ions, Inorg. Chem. 56 (2017) 7566–7573, https://doi.org/10.1021/ACS.INORGCHEM.7B01205.
[30] Y. Marcus, Tetraalkylammonium Ions in Aqueous and Non-aqueous Solutions, J. Solution Chem. 37 (2008) 1071–1098, https://doi.org/10.1007/S10953-008-9291-1.
[31] J.A. Peck, C.D. Tait, B.I. Swanson, G.E. Brown, Speciation of aqueous gold(III) chlorides from ultraviolet/visible absorption and Raman/resonance Raman spectroscopies, Geochim. Cosmochim. Acta. 55 (3) (1991) 671–676, https://doi.org/10.1016/0016-7037(91)90332-Y.
[32] D. Dupont, D. Depuydt, K. Binnemans, Overview of the effect of salts on biphasic ionic liquid/water solvent extraction systems: anion exchange, mutual solubility, and thermomorphic properties, J. Phys. Chem. B. 119 (2015) 6747–6757, https://doi.org/10.1021/ACS.JPCB.5B02980.
[33] P. Naert, K. Rabaey, C.V. Stevens, Ionic liquid ion exchange: exclusion from strong interactions condemns cations to the most weakly interacting anions and dictates reaction equilibrium, Green Chem. 20 (2018) 4277–4286, https://doi.org/10.1039/C8GC01869C.
[34] M.J. Taylor, J.M. Coddington, The constitution of aqueous tin(IV) chloride and bromide solutions and solvent extracts studied by 119Sn NMR and vibrational spectroscopy, Polyhedron. 11 (1992) 1531–1544, https://doi.org/10.1016/S0277-5387(00)83148-4.
[35] R.M. Cigala, F. Crea, C. De Stefano, G. Lando, D. Milea, S. Sammartano, The inorganic speciation of tin(II) in aqueous solution, Geochim. Cosmochim. Acta. 87 (2012) 1–20, https://doi.org/10.1016/J.GCA.2012.03.029.
[36] P.H. van Wyk, W.J. Gerber, K.R. Koch, A robust method for speciation, separation and photometric characterization of all [PtCl6−nBrn]2− (n = 0–6) and [PtCl4−nBrn]2− (n = 0–4) complex anions by means of ion-pairing RP-HPLC coupled to ICP-MS/OES, validated by high resolution 195Pt NMR spectroscopy, Anal. Chim. Acta. 704 (2011) 154–161, https://doi.org/10.1016/J.ACA.2011.07.037.
[37] P. Halli, V. Agarwal, J. Partinen, M. Lundström, Recovery of Pb and Zn from a citrate leach liquor of a roasted EAF dust using precipitation and solvent extraction, Sep. Purif. Technol. 236 (2020), 116264, https://doi.org/10.1016/J.SEPPUR.2019.116264.
[38] T. Kinoshita, S. Akita, N. Kobayashi, S. Nii, F. Kawaizumi, K. Takahashi, Metal recovery from non-mounted printed wiring boards via hydrometallurgical processing, Hydrometallurgy 69 (2003) 73–79, https://doi.org/10.1016/S0304-386X(03)00031-8.
[39] S.Y. Chang, A. Uehara, S.G. Booth, K. Ignatyev, J.F.W. Mosselmans, R.A.W. Dryfe, S.L.M. Schroeder, Structure and bonding in Au(i) chloride species: a critical examination of X-ray absorption spectroscopy (XAS) data, RSC Adv. 5 (2014) 6912–6918, https://doi.org/10.1039/C4RA13087A.
[40] M. Mon, J. Ferrando-Soria, T. Grancha, F.R. Fortea-Pérez, J. Gascon, A. Leyva-Pérez, D. Armentano, E. Pardo, Selective gold recovery and catalysis in a highly

flexible methionine-decorated metal-organic framework, J. Am. Chem. Soc. 138 (2016) 7864–7867, https://doi.org/10.1021/JACS.6B04635.
[41] C. Wang, C. Xiong, X. Zhang, Y. He, J. Xu, Y. Zhao, S. Wang, J. Zheng, External optimization of Zr-MOF with mercaptosuccinic acid for efficient recovery of gold from solution: adsorption performance and DFT calculation, Sep. Purif. Technol. 296 (2022), 121329, https://doi.org/10.1016/J.SEPPUR.2022.121329.
[42] M.D. Rao, K.K. Singh, C.A. Morrison, J.B. Love, Recycling copper and gold from e-waste by a two-stage leaching and solvent extraction process, Sep. Purif. Technol. 263 (2021), 118400, https://doi.org/10.1016/J.SEPPUR.2021.118400.
[43] S. Raiguel, L. Gijsemans, A. Van Den Bossche, B. Onghena, K. Binnemans, Solvent Extraction of Gold(III) with Diethyl Carbonate, ACS Sustain. Chem. Eng. 8 (2020) 13713–13723, https://doi.org/10.1021/ACSSUSCHEMENG.0C04008.
[44] M. Bae, J.-C. Lee, H. Lee, S. Kim, Recovery of nitric acid and gold from gold-bearing aqua regia by tributyl-phosphate, Sep. Purif. Technol. 235 (2020) 116154.
[45] J. Zhou, H. Sui, Z. Jia, Z. Yang, L. He, X. Li, Recovery and purification of ionic liquids from solutions: a review, RSC Adv. 8 (2018) 32832–32864, https://doi.org/10.1039/C8RA06384B.
[46] MacroTrends, Gold Prices - 100 Year Historical Chart., (n.d.). https://www.macrotrends.net/1333/historical-gold-prices-100-year-chart (accessed January 31, 2023).
[47] Alibaba, Tetrabutylammonium salt., (2023). alibaba.com (accessed January 31, 2023).
[48] M. Gras, N. Papaiconomou, N. Schaeffer, E. Chainet, F. Tedjar, J.A.P. Coutinho, I. Billard, Ionic-liquid-based acidic aqueous biphasic systems for simultaneous leaching and extraction of metallic ions, Angew. Chemie - Int. Ed. 57 (6) (2018) 1563–1566, https://doi.org/10.1002/anie.201711068.